

A Novel Method for Skin Lesion Segmentation

Fatima Rashid Sheykhahmad

Young Researchers and Elite club,
Electronic Branch, Islamic Azad
University, Tehran, Iran

Navid Razmjooy

Department of Electrical
Engineering, University of Tafresh,
Tafresh, Iran.

Mehdi Ramezani

Department of Mathematics,
University of Tafresh, Tafresh, Iran

ABSTRACT

Skin cancer has been the most usual and illustrates 50% of all new cancers detected each year. If they detected at an early stage, treatment can become simple and economically. Accurate skin lesion segmentation is important in automated early skin cancer detection and diagnosis systems. The aim of this study is to provide an effective approach to detect the skin lesion border on a purposed image. A novel method based on image processing is proposed that combines the edge detection and the thresholding technique for skin lesions detection from skin region in an image. The distributions of edge and the proposed thresholding method provide a good discrimination of skin lesions. The evaluation of the proposed method is based on the comparison with the Otsu and Rosin segmentation as the most application methods. The performance of the designed system is evaluated with 30 test images, and the experimental results demonstrate the effectiveness of the proposed mole localization scheme.

Keywords

Computer-aided lesion diagnosis; Segmentation; Hair Removal; Median Filter; Boundary Detection; Symmetry.

1. Introduction

There are many different types of skin cancer, and of the most dangerous among them is Melanoma, caused from unprotected high exposure to UV radiation; Melanoma accounts for less than 5% of skin cancer cases. But it causes most skin cancer deaths [1]. The number of new cases of melanoma in the United States has been increasing for at least 30 years. Overall, the lifetime risk of getting melanoma is about 1 in 50 for whites, 1 in 1,000 for blacks, and 1 in 200 for Hispanics. The dramatically increasing incidence rate of cutaneous melanoma has prompted doctors and specialists to investigate the lesion condition in its early, curable phase. Fortunately, early detection of this skin cancer can improve the cure rate. [2]. While it is not the most common of the skin

cancers, it causes the most deaths. The American Cancer Society [3] guesstimates that at present, about 70,230 new cases of melanoma and About 8,790 deaths from melanoma in the US are diagnosed in year 2011.

Clinical features of pigmented lesions suggestive of melanoma are what are known as the ABCDs of melanoma [4, 5]: asymmetry, border irregularity, color variegation, and diameter greater than 6 mm. The **ABCD** criteria developed by the American Cancer Society provide a starting-off point for the physician and an easily remembered guideline for the patient to use in self-examination for MM. Experts, using these symptoms (known as ABCD rule), can recognize the melanoma. To compute the ABCD score, the criteria are assigned semi-quantitatively. Each of the criteria is then multiplied by a given weight factor to outcome a total dermoscopy score [6]. The ABCD rule works properly for thin melanocytic wounds. These rules have 59% to 88% accuracy in diagnosing melanoma, but biopsy is needed for more precise diagnosis [7]. Correct measurement of image characteristics for diagnosis of melanoma first needs a proper detecting of lesions. It is significant that lesion boundaries are determined accurately so that measurements, like maximum diameter, asymmetry, irregularity of the boundary, and color characteristics can be accurately calculated.

Different image segmentation methods have been improved for specifying lesion boundaries; color and texture information are two characteristic examples which have used to find the lesion boundaries.

In 2011, Abbas. Q et al. used least-squares method (LSM) to acquire edge points from the lesion image after artefact removing and then a dynamic programming (DP) technique used to find the optimal boundary of the lesion [8].

In 2009, celebi et al. proposed the use of an objective measure, the Normalized Probabilistic Rand Index, which takes into account variations in the ground-truth. The results showed that the differences between four of the appraised border detection methods were in fact smaller than those predicted by the commonly used XOR measure [9]. Ivatomi

et al. [10] automatically extracted a dermatologist-like lesion region by joining pixel-based and region-based algorithms which recline the approximation of the color distributions of normal skin and pigmented lesion.

Ganster et al. [11] combined global thresholding, dynamic thresholding, and 3-D color clustering along with a fusion strategy to detect lesion borders and achieved a performance of 96% on a set of 4000 images. In 2004, zagrouba and barhoumi motivated by the desire to classify skin lesion from color images; they used a fuzzy classifier after smoothing to classify the images and attained a 79.1% accuracy for correct classify of lesions [12].

Orientation sensitive Fuzzy c-mean [12], Density Based Spatial Clustering of Application with Noise [13], and JSEG [14] are examples of applying clustering algorithms in lesion segmentation.

2. Data Description

Different lesion images from various references [11] [15] [16] [17] are used in this work. Our dataset consists of 60 lesion images captured by the same Nevoscope device under lighting conditions. The size of all dataset's images was resized to a spatial resolution of 256×256 pixels using *bicubic* interpolation to reduce the computational resources needed for processing the images. However, segmentation is difficult because of the wide range of lesion shapes and colors and also different skin tones. Finally, to suppress large variations within the background and the lesion, and to decrease the effect of different skin color variations, the original color (RGB) images are transformed into intensity (grayscale) ones. The separate values of the three color channels (R, G, and B) are combined to produce an intensity image (gray) using a commonly accepted transformation as below:

$$gray = 0.2989 \times R + 0.5870 \times G + 0.1140 \times B$$

Fig.1 shows these diversities of different lesions:

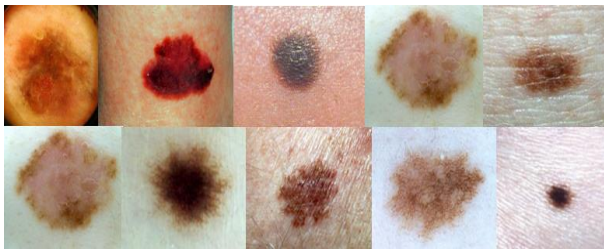


Fig.1. Diversity of lesion images.

3. Material and Methods

Fig.2 summarizes the pipeline of our skin lesion segmentation process. The inputs to the algorithm include different images. As we can see in fig.2, a median filter is used to remove extras like scales on the lesion image and some of the artefacts. After that, a simple and proper hair remove applied to the image (note that fig.3 needs no hair removing). Next step is to detect lesion borders on the image; for do this, after contrast improvement, the peak point of the histogram is found and then produced by a dynamic triangular function which changes due to different contrasts

and histograms. Some morphological operations are then implemented to the result image. In the next step, using morphological remove, the boundary of the lesion is detected. Finally a simple back removal showed the result.

3.1 Median Filtering

A median filter is, as the name suggests, support on finding the median of a set of numbers. As most noise-removing filters, median filters are low-pass filters. A low-pass filter is a filter that passes low-frequency signals, but declines the amplitude of signals with high frequency. The median filter replaces the current pixel by the median of the neighbouring pixels, including the current pixel.

$$y[m, n] = \text{median}\{x[i, j], (i, j) \in \omega\}$$

where ω represents a neighbourhood centered around location (m, n) in the image [18]. The median filter considers each pixel in the image in turn and looks at its nearby neighbours to determine whether it is representative of its surroundings or not. The median is calculated by first sorting all the pixel quantities from the inclosing neighbourhood into numerical order and then replacing the pixel being regarded with the middle pixel quantity [19], [20].

The neighbourhood can be of any size and shape, but for noise removing it will normally be a square or a disk. As always, a correct choice of parameters is important, in this case the size and the shape of the neighbourhood. If the neighbourhood is too big, even a median filter will smooth the edges; a neighbourhood too small will not remove enough noise. Objects that are smaller than the neighbourhood can be totally removed when using a median filter.

In this paper, a non-linear filter assigns to each pixel the median pixel-value over a neighborhood of a given size. This filter reduces the effect of small structures, like hair, and scale lines on the segmentation result. The neighborhood used for the median filter depends on the image resolution. In this work, 11×11 neighborhood by disk shape has been used for images of size 256×256 pixels showing a complete skin lesion. Trials and errors showed that even if the lesions vary in size, this value can be kept fixed. Fig.3 shows an image smoothing by the median filter; as it can be seen, scales are removed by this method and just hairs are still remained which can be removed by the next week.

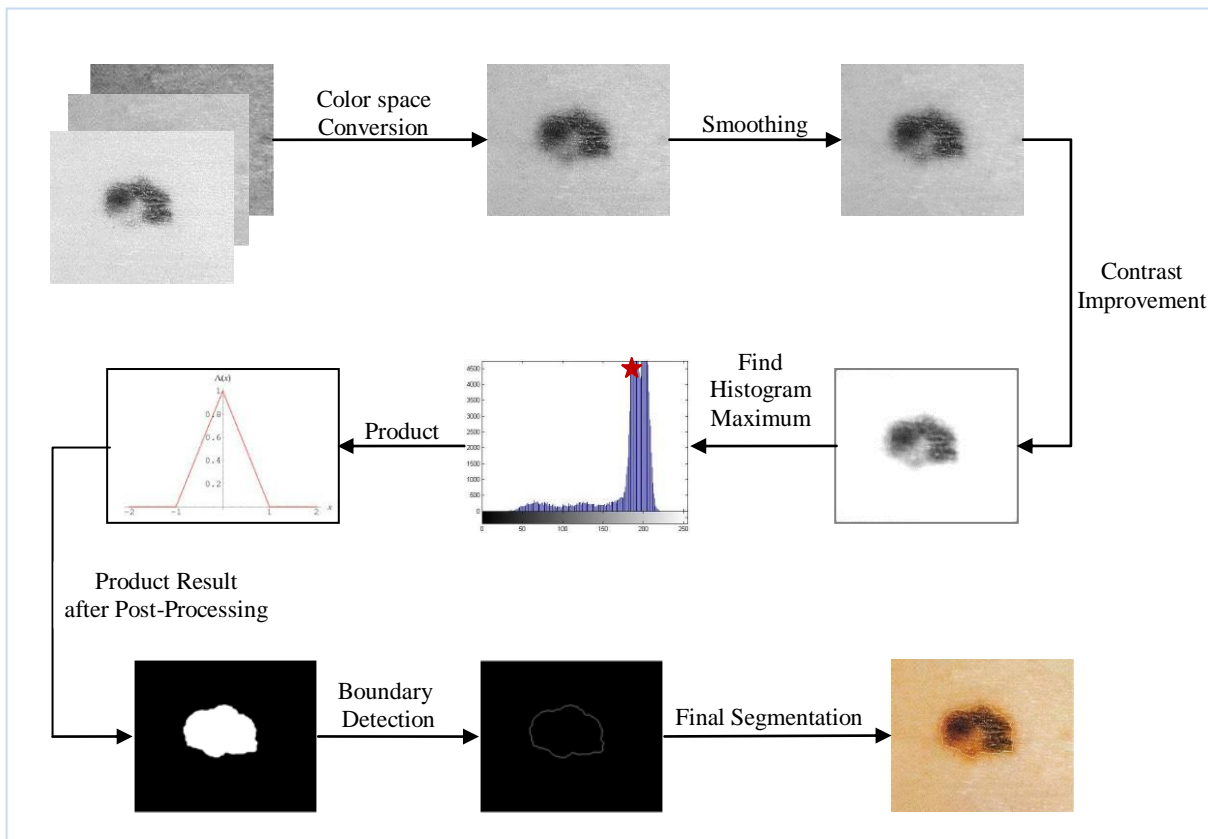


Fig.2 The flowchart system overview

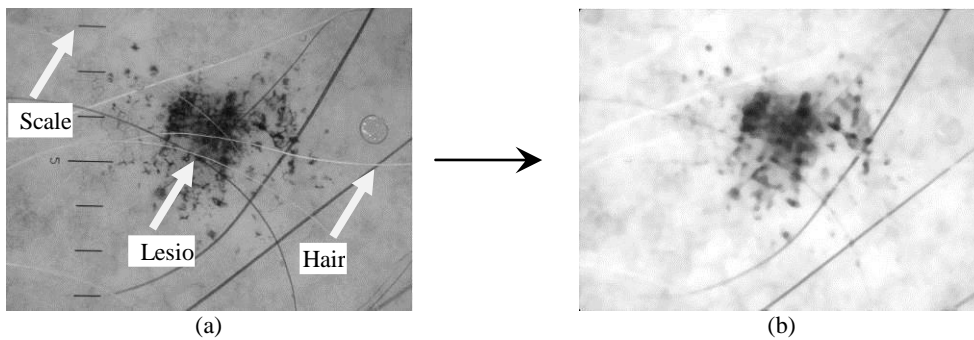


Fig.3 Image before (a) and after (b) filtering

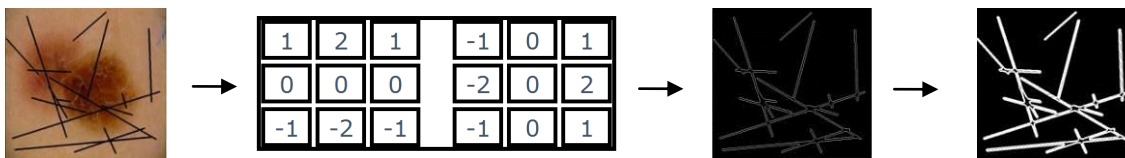


Fig.4 Horizontal and Vertical sobel filter applied to the input image

3.2. Hair Removal

After smoothing the image, for a perfect hair removal some operations are applied as below:

A simple *sobel* edge detector in both vertical and horizontal directions is implemented (after binarization) to detect the high frequency pixels which are usually comprise artefact pixels; After that, morphology dilation is applied for thickening the found edges Fig.4 shows the results.

Finally, the founded edges get smoothen by median filter and apply to the original image. Two example of the artifact removing is shown below:

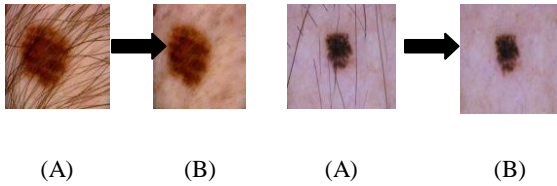


Fig.5. Artifact Removal Results: (A) original image, (B) image after artefact removal.

3.2 contrast improvement

a simple coefficient equal to 1.5 is then product to the result image from section 3.2 to improve the intensity and simplify the operations.

3.3 Lesion Border Detection

Initial tests with a training set consisting of a subset of 15 randomly selected input lesion images showed that a proper divider can separate the skin lesions from the background; some of the different of dataset and their histograms are shown below:

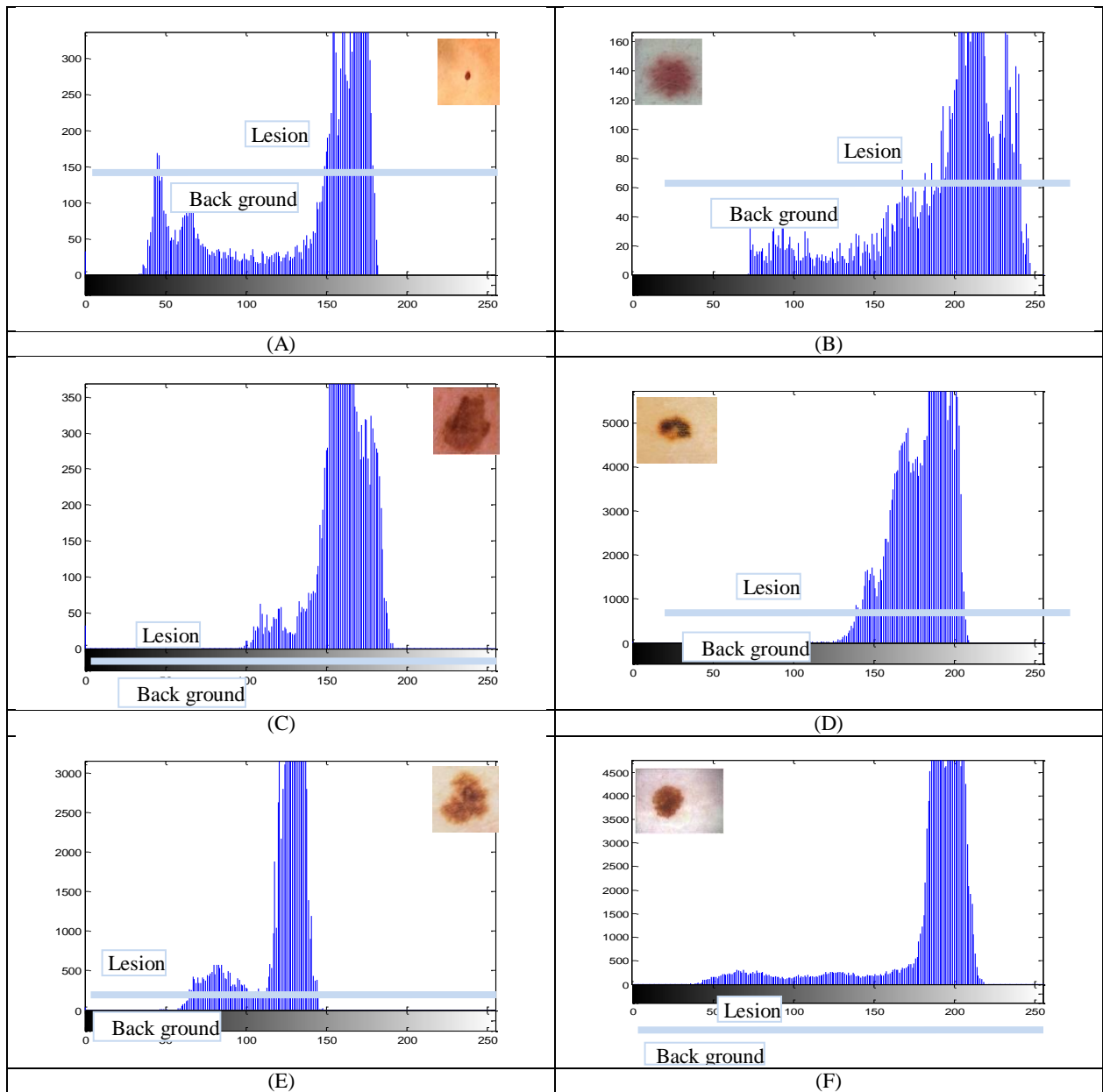


Fig.6. different lesion dataset and their histogram

The principal idea of this technique is to enhance the edges on the lesion boundary, while suppressing the gradients inside the lesion and in the background. This is executed using a triangular curve function for remapping the image intensity values; the triangular curve is a function of a vector, x , and depends on three scalar parameters a , b , and c , as given by [21]:

$$f(x; a, b, c) = \begin{cases} 0, & x \leq a \\ \frac{x-a}{b-a}, & a \leq x \leq b \\ \frac{c-x}{c-b}, & b \leq x \leq c \\ 0, & c \leq x \end{cases} \quad (3)$$

or, more compactly, by:

$$f(x; a, b, c) = \max\left(\min\left(\frac{x-a}{b-a}, \frac{c-x}{c-b}\right), 0\right) \quad (4)$$

where $f(x; a, b, c)$ and x are pixels in the output and input image, respectively. The parameters a and c locate the "feet" of the triangle for the input intensity and the parameter b locates the peak of the image. Therefore, a significant step in this method is to correctly identify the whole pick 'b' and its feet 'a', 'c'. The effect of the triangular pick on the mapping of the lesion boundary is shown in Figure 7, which shows that if the average intensity of the boundary pixels in the input image is mapped closer to the pick and its feet, then the boundary pixels in the output image would have a wider intensity range.

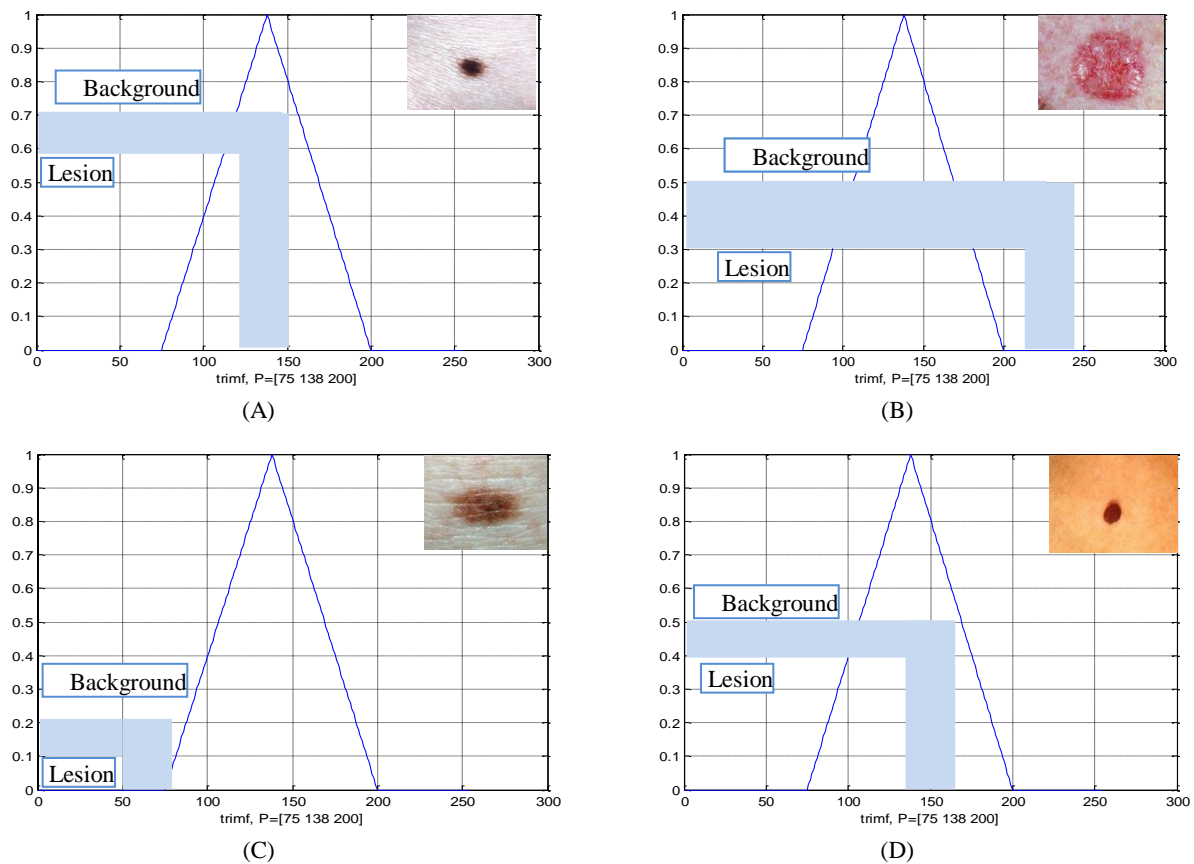


Fig.7. The effect of a fixed triangular function on the mapping of the different lesion boundaries

From the above, it can be seen that if we have a product between triangular function and the input image, (A) and (D) show a good thresholding; but this technique is get complicated while the different contrast and dataset; as an example, if we have a product between triangular function and one of the (B) or (C), the lesion information will be lost completely; since a dynamic value of pick 'b' is need for different dataset.

In order to fig.6, it is clear that just two significant intensities are lesion and background and the others can be neglected; it can also be described that using a suitable point will be segment the lesion and background perfectly. In this manner, regard to trials and errors, if we can find the maximum value (pick) intensity and product it by the triangular function by the pick value 'b' equal to the maximum value and $0.2a$ from its feet (a is the integer value which is 255 for this work (unit8)), good result outcomes which separates the lesion and background completely. Fig.8 shows some results of such product.

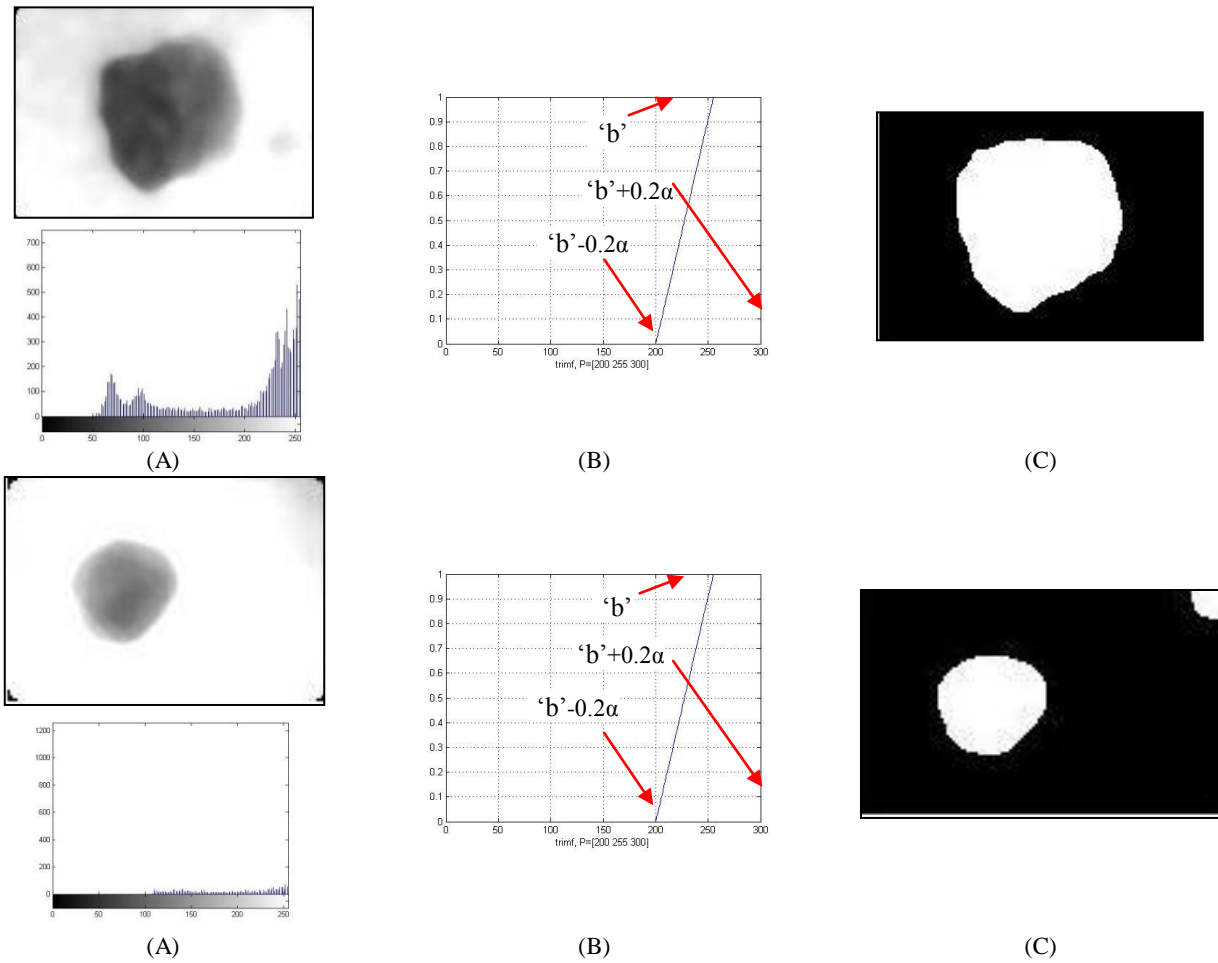


Fig.8. triangular product: (A) image after pre-processing and contrast improvement, (B) dynamic triangular function regard to histogram, (C) result image from product between input image and dynamic triangular function.

From fig.8 because the maximum value of both examples is on the 255, the pick value 'b' is selected as 255, and follow the presented discussion, its feet 'a' and 'c' are 0.2α (α is 255 in this work) distance from the picks neighbour which means: 'a'=200 and 'c'=300. Note that the second example has a fault in detection and detect the high shadow as the lesion 'b'- 0.2α

3.4 Morphological Operations

After binary images have been extracted from the fabric image, morphological filters can be designed to eliminate extra parts. Mathematical morphology or simply morphology has been identified as a technique for the analysis of spatial structures [22]. The set theory includes the language of mathematical morphology. Sets in mathematical morphology represent objects in an image. In binary images, the sets in question are participant in the 2-D integer space Z^2 where each element of a set is a 2-D vector whose coordinates are the(x, y) coordinates of a black or white pixel in the image [23]. Three morphological operations, closing, region filling and area open, were used in order to remove extra objects [24]. Region filling had to be adapted. The algorithms for

region filling are based on set dilation, complementation, and intersections, are shown as:

$$\mathcal{R}_k = (X_{k-1} \oplus B) \cap A^c, k=1,2,\dots \quad (5)$$

Where A is a set of boundary and B is structuring element. The algorithms terminate at iteration step k if $X_k = X_{k-1}$.

Closing typically makes counters smooth, fuses narrow breaks, and long thin gulfs, eliminates small holes, and fills gaps in the contour. The closing of set A by structuring element B, denoted $A \bullet B$, is defined and mixes thin distances as:

$$A \bullet B = (A \oplus B) \ominus B \quad (6)$$

Closing might result in amalgamations of disconnected components, consequently, generating new holes. The opening of A by B is obtained by the erosion of A by B, followed by dilation of the resulting image by B. It is shown as follows:

$$A \circ B = (A \ominus B) \oplus B \quad (7)$$

The purpose of area open is to eliminate small area like shadows which should be ignored by the lesion processing industries. After 3 main morphology operations, by using the morphological *remove*, interior pixels removed. This option sets a pixel to 0 if all its 4-connected neighbours are 1, thus

leaving only the boundary pixels on. However, the morphological operations help to define the image contours and eliminate or reduce noise (undesired speckles outside the contour of the object). In this work, structuring element is a disk-shaped and structuring element with radius 6. Fig.9 shows a simple example of such operation:

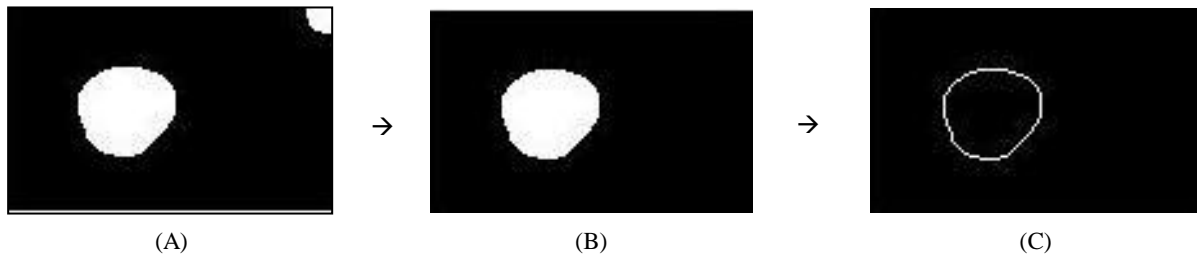


Fig.9. image before (A) and after (B) opening, closing and filling morphology implementation; (C) shows the remove interior pixels using the morphological remove.

After mathematic morphology, a simple summing between input image and the boundary image, result the final purpose. A type of such operation is shown below:

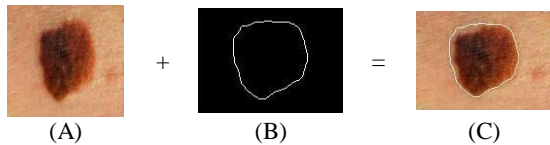


Fig.10. Summing the input image (A) by the obtained boundary using the proposed method (B); (C) is the final result (C=A+B)

4. Experimental results

The proposed lesion detection algorithm has been validated with 30 256x256 pixels skin lesion images under *Matlab* environment [25]. The experiment result of *lesion*

segmentation method is then compared by Otsu [26] and rosin [27] methods; these two methods are some olds but because of their ability, they are still used in more researches. Fig.11 shows segmentation and boundary detection results for 3 presented methods; fig 11.a shows a special lesion which is detected by all segmented methods, but it is noticeably that the proposed method could segment whole boundaries, while two other methods segments the lesion by a definite error rate. Fig.11.b shows a different state; in this lesion image, proposed method could detect the lesion but by some errors (shadow intensity is detected as a part of skin lesion), otsu's method is also loose in this object in order to improper boundarization, rosin's get also the worst result for the identified object. The last case is fig.11.c; in this case all the methods could detect the skin lesion properly. Since from fig.11.b it can be result that finding a proper colorspace can improve the proposed method's performance.

	Original Image	Proposed	Edge-Otsu[26]	Edge-Rosin[27]
(a)				
(b)				
(c)				

Fig.11. Input image and thresholding with Proposed, Otsu's and rosin's method

A number of measurements can be used to evaluate the segmentation accuracy:

$$\text{Sensitivity} = \frac{TP}{TP + FN} \quad (8)$$

$$\text{Specificity} = \frac{TN}{TN + FP} \quad (9)$$

$$\text{Positive.Predictive.Value} = \frac{TP}{TP + FP} \quad (10)$$

$$\text{Negative.Predictive.Value} = \frac{TN}{TN + FN} \quad (11)$$

$$\text{Index.of.Suspicion} = \frac{TP + FP}{TP + FN} \quad (12)$$

$$\text{Diagnostic.Accuracy} = \frac{TP}{TP + FP + FN} \quad (13)$$

where TP is the number of true positives, FN the number of false negatives, TN the number of true negatives, and FP the number of false positives. A positive is a part that is classified as lesion. The sensitivity and specificity measure the percentages of accurate classifications for the lesion and skin cases, respectively. The positive predictive value is the proportion of lesions classified as lesion that are really lesion, and inversely for the negative predictive value. The index of suspicion gives the degree of awareness of the likelihood of a lesion to be a lesion. An index higher than 100% represents an over-diagnosis while an index lower than 100% represents under-diagnosis. The diagnosis accuracy shows the loss of accuracy due to misclassified elements. Table 1 shows the different classification accuracy indices for three combinations of segmentations: Proposed method, Otsu and Rosin.

Table.1. Segmentation symmetry values for lesion segmentation

Symmetry Features	Proposed	Edge-Otsu's	Edge-Rosin's
Sensitivity (%)	48.4	40.6	55
Specificity (%)	57.1	87.5	45
Positive predictive value (%)	35	92.8	50
Negative predictive value (%)	19	26.9	50
Index of suspicion (%)	57.5	43.7	110
Diagnostic accuracy (%)	44.4	39.3	35.5

These results show that the proposed method improves the separation between lesion and skin. Proposed and Otsu are especially proper result, while the Rosin's but does not improve the results significantly, also has an under-diagnosis.

5. Conclusions

The physical examination of the skin and its appendages, as well as the mucous membranes, forms the cornerstone of an accurate diagnosis of cutaneous conditions [28]. Most of these conditions present with cutaneous surface changes termed "lesions," which have more or less distinct characteristics [29]. Due to the difficulty and subjectivity of human interpretation, computerized analysis of lesion images has become an important research area. One of the most important steps in lesion image analysis is the automated detection of lesion borders. In this paper, we proposed a novel approach to lesion boundary detection in order a new global processing; our method is a new model of thresholding in

global. The success rate of *correct segmentation* of the proposed techniques is in the order of 80% for a complex dataset from different references.

References

- [1] Detmar M., "Tumor angiogenesis", J. *Investig. Dermatology Symp. Proc.*, vol. 5, 20-23, 2000.
- [2] Gee M. S., Saunders H. M., Lee J. C., Sanzo J. F., Jenkins W. T., Evans S. M., Trinchieri G., Sehgal C. M., Felman M. D., and Lee W. M., "Doppler ultrasound imaging detects changes in tumor perfusion during antivascular therapy associated with vascular anatomic alterations", *Cancer research*, vol. 61, 2974-2982, 2001.
- [3] <http://www.cancer.org/Cancer/SkinCancer-Melanoma/OverviewGuide/melanoma-skin-cancer-overview-key-statistics>
- [4] Vincent T.Y. Ng; Benny Y.M. Fung; Tim K.Lee "Determining the asymmetry of skin lesion with fuzzy borders" *Computers in Biology and Medicine* 35 (2005) 103–120.
- [5] Nachbar F., Stolz W., Merkle T., Cagnetta A. B., Vogt T., Landthaler M., Bilek P., Braun-Falco O., and Plewig G., "The ABCD rule of dermatoscopy. High prospective value in the diagnosis of doubtful melanocytic skin lesions", *J. Am Acad. of Dermatology*, vol. 30, no. 4, 551-559, 1994.
- [6] Sachin V; Patwardhan; Shuangshuang Dai; Atam P. Dhawan. "Multispectral image analysis and classification of melanoma using fuzzy membership based partitions". *Computerized Medical Imaging and Graphics* 29 (2005) 287–296 elsevier.
- [7] Sachin V.Patwardhan,Atam P.Dhawn,Patricia A.Relue, "classification of melanoma using tree structured wavelet transforms" *Computer Methods and Programs in Biomedicine* 72 (2003) 223-239 Elsevier.
- [8] Qaisar Abbas, M. Emre Celebi, Irene Fondón García, Muhammad Rashid," Lesion border detection in dermoscopy images using dynamic programming", *John Wiley & Sons A/S, Volume 17, Issue 1, pages 91–100, February 2011*
- [9] M. E. Celebi, G. Schaefer, H. Iyatomi, W. Stoecker, J. Malters, and J. Grichnik, "An improved objective evaluation measure for border detection in dermoscopy images," *Skin Research and Technology*, vol. 15, no. 4, pp. 444–450, 2009.
- [10] Iyatomi, H. Oka, H. Saito, M.: Quantitative assessment of tumour area extraction from dermoscopy images and evaluation of the compute-based methods for automatic melanoma diagnostic system. *Melanoma Research* 16(2), 183—190, 2006.
- [11] Ganster H., Pinz A., Rohrer R., Wildling E., Binder M., and Kittler H., "Automated Melanoma Recognition", *IEEE Trans. on Med. Imaging*, vol. 20, no. 3, 233-239, 2001.
- [12] Ezzeddine zagrouba and Walid barhoumi, "a preliminary approach for the automated recognition of malignant melanoma ", *image anal stereol*, 23, pp.121-135, 2004.
- [13] M. E. Celebi, Y. A. Aslandogan, P. R. Bergstresser, Mining biomedical images with density-based clustering, in: *International Conference on Information Technology*:

- Coding and Computing, ITCC 2005, Proceedings, IEEE, 2005.
- [14] M. E. Celebi, Y. A. Aslandogan, P. R. Bergstresser, Unsupervised border detection of skin lesion images, in: International Conference on Information Technology: Coding and Computing, ITCC 2005, Proceedings, IEEE, 2005.
- [15] <http://dermnetnz.org/doctors/dermoscopy-course/reticular-images.html>
- [16] <http://akiavintage.com/basal-skin-cancer-symptoms-and-treatment.html/basal-skin-cancer-pictures-image5>
- [17] <http://www.healthhype.com/types-of-skin-cancer-pictures-and-treatment.html>
- [18] G.R. Arce, "Nonlinear Signal Processing: A Statistical Approach", Wiley: New Jersey, ISBN: 978-0-471-67624-9, USA, 2005.
- [19] Chaohong Wu, Zhixin Shi _ and Venu Govindaraju, "Fingerprint Image Enhancement Method Using Directional Median Filter", Preprint submitted to Elsevier Science, 2004.
- [20] E. Davies, "*Machine Vision Theory, Algorithms and Practicalities (signal processing and its applications)*", ISBN: 0122060938, Morgan Kaufmann, USA, 2005.
- [21] R.C. Gonzalez, R.E. Woods. *Digital Image Processing*. Addison Wesley Publishing Company, 1993.
- [22] P. Soille, *Morphological Image Analysis*, second ed., Springer, 2003.
- [23] K.L. Mak, P. Peng, K.F.C. Yiu, "Fabric defect detection using morphological filters", *Image and Vision Computing*, vol 27, pp.1585–1592, 2009.
- [24] Chih-Chin, "A Novel Image Segmentation Approach Based on Particle Swarm Optimization", *IEICE TRANS. FUNDAMENTALS, VOL.E89–A, NO.1 JANUARY*, pp. 324-327, Tainan, 2006.
- [25] Matlab Tutorial, Mathworks, 2007.
- [26] N. Otsu, "A Threshold Selection Method from Gray-Level Histograms", *IEEE Trans. on Systems, Man, and Cybern.* vol. SMC- 9, 1979, pp. 62-66.
- [27] Venkatesh, S. and P. Rosin (1995). Dynamic threshold determination by local and global edge evaluation. *ComputerVision, Graphics and Image Processing* 57(2), 146–160.
- [28] Callen, Jeffrey (2000). *Color atlas of dermatology*. Philadelphia: W.B. Saunders. ISBN 0-7216-8256-1.
- [29] James, William D.; et al. *Andrews' Diseases of the Skin: Clinical Dermatology*. Saunders Elsevier. ISBN 0-7216-2921-0, 2006.